Life Sciences 242 (2020) 117149

Contents lists available at ScienceDirect

Life Sciences

journal homepage: www.elsevier.com/locate/lifescie

Targeting Wistar rat as a model for studying benign, premalignant and malignant lesions of the prostate

Gabriel H. Campolina-Silva[a,1], Hipácia Werneck-Gomes[a,1], Bruna T. Maria[a], Maria C. Barata[a], María J. Torres[b], Héctor R. Contreras[b], Germán A.B. Mahecha[a], Cleida A. Oliveira[a,*]

[a] Department of Morphology, Universidade Federal de Minas Gerais, Belo Horizonte, Brazil
[b] Department of Basic and Clinic Oncology, Universidad de Chile, Santiago, Chile

ARTICLE INFO

Keywords:
Prostate lesions
Adenocarcinoma
Aging
Androgen:estrogen imbalance
Wistar rat

ABSTRACT

Aims: The purpose of this study was to describe a suitable experimental model for studying aging-related prostate disorders including cancer.
Materials and methods: 12-month old Wistar rats were kept in control conditions ($n = 12$) or treated ($n = 16$) for 6 months with Silastic implants filled with testosterone (T) and estradiol (E_2). After the experiment period (at 18 months of age), animals were euthanized and the prostate and other organs were harvested, dissected, weighed, and processed for morphological, ultrastructural and molecular analyses.
Key findings: We demonstrated that male rats of Wistar strain nicely recapitulate the carcinogenesis process taking place in the aging prostate through the arising of benign, precancerous and malignant lesions, and above all yields a modest incidence of spontaneous PCa (~36%). Moreover, our results highlight that 100% incidence of PCa and precancerous lesions such as prostatic intraepithelial neoplasia and proliferative inflammatory atrophy were achieved in this rat strain after T + E_2 treatment, without changing the broad spectrum of changes that naturally emerge in the prostate at advanced ages. Such enhancement of precancerous lesions and tumors was linked to a decreased expression of E-cadherin and β-catenin in parallel with an increase in Vimentin and N-cadherin, hallmark modifications of epithelial-mesenchymal transition.
Significance: Our findings provide solid evidence that aged Wistar rats may be an excellent model for studies regarding human prostate biology and related disorders including cancer.

1. Introduction

Living long enough, nearly all men will develop some histologically detectable alteration in the prostate. This fact puts the advancing age as the major risk factor for some prostate diseases including the prostate cancer (PCa), one of the most frequently diagnosed neoplasms worldwide and whose incidence raises sharply from the 4th decade of life [1,2]. The relationship between aging and the prostate diseases likely reflects an exacerbation of factors that influence the gland throughout life, particularly the increased androgen:estrogen ratio [3–8]. In this regard, researches conducted in rats have shown that the chronic exposure to androgenic and estrogenic compounds strongly predisposes the prostate gland to develop dysplastic foci and adenocarcinomas at senescence [9–15].

The use of laboratory rodents in experimental research has expressively advanced our comprehension of PCa biology. Since the arising of precancerous lesions and the eventual detection of tumors in the prostate gland is a long and silent process, preclinical investigations performed in spontaneous models of PCa are assumed to be time-consuming and still have to cope with the relatively low incidence of tumors [16]. Furthermore, the incidence of spontaneous PCa varies according to animal strain [3,17,18]. Thus, efforts have been employed over the last decades to design in vivo models capable of yielding a high frequency of prostate tumors in a shorter period of time. These models include rats or mice that undergo chemical, genetic or tissue recombinant interference (reviewed by [16,19]), which have been applied to generate new insights into the initiation, progression, and treatment of PCa. However, the adoption of contrived and highly abnormal conditions to truncate the long latency period needed for PCa development does not precisely provide the ideal properties to mimic the natural history of the disease [20]. Therefore, defining new PCa models that yield a high incidence of malignant lesions spontaneously

* Corresponding author at: Av. Antônio Carlos, 6627, CEP 31270-901 Belo Horizonte, MG, Brazil.
E-mail address: cleida@icb.ufmg.br (C.A. Oliveira).
[1] These authors should be regarded as joint First Authors.

https://doi.org/10.1016/j.lfs.2019.117149
Received 9 October 2019; Received in revised form 29 November 2019; Accepted 6 December 2019
Available online 09 December 2019

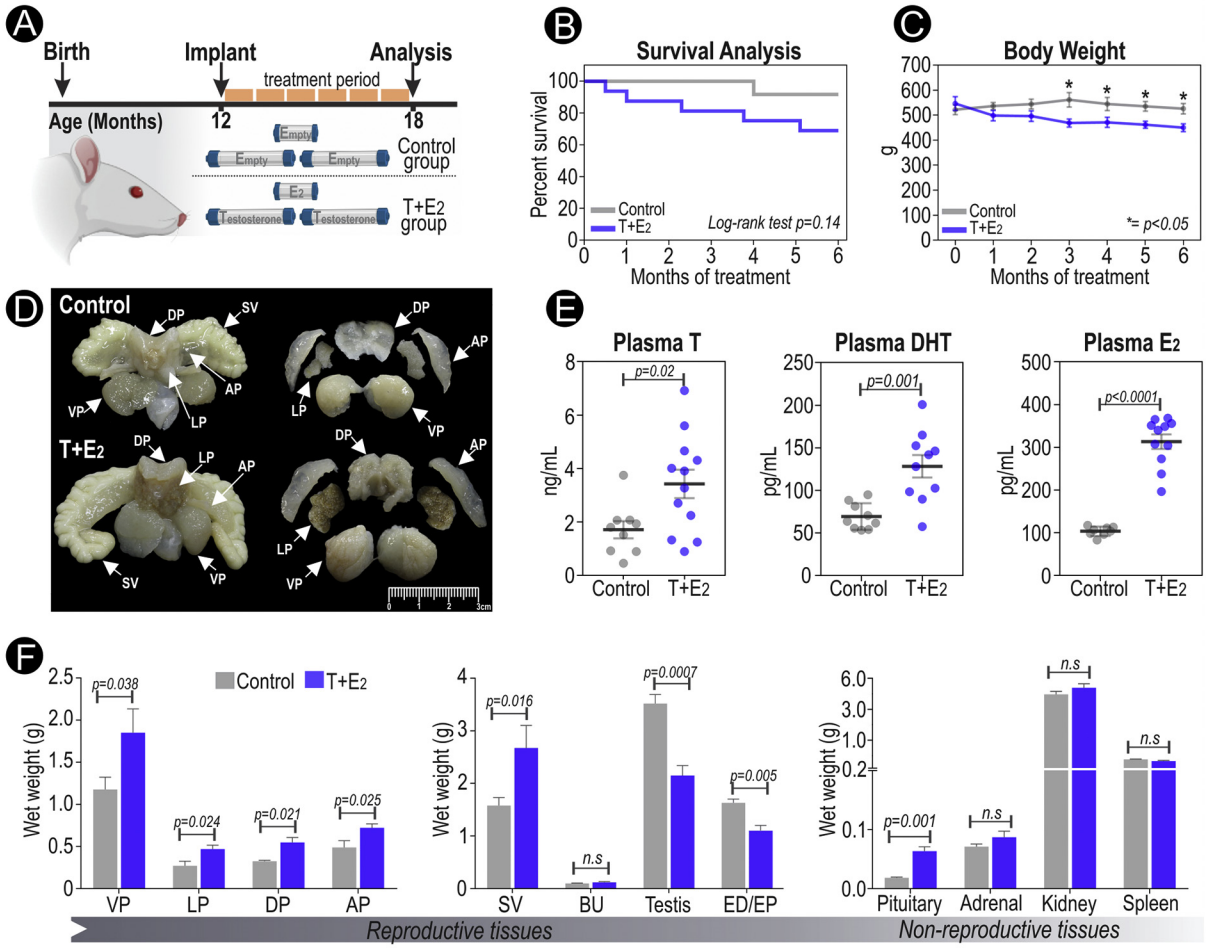

Fig. 1. Testosterone plus E_2 treatment induces significant structural changes in the rat prostate at 18 months of age. (A) Experimental design. (B) Kaplan-Meier plot showing statistically similar survival curves between groups. (C) Progressive weight loss in the T + E_2-treated animals over the experiment course. (D) Gross morphology of whole prostatic complex with seminal vesicles and each dissected prostate lobe highlighting the difference in the size and appearance between groups. (E) Scatter plots showing the circulating level of testosterone, dihydrotestosterone, and estradiol. (F) Wet weights of reproductive and non-reproductive organs. All paired organs were weighted together. AP: anterior prostate. DP: dorsal prostate. LP: lateral prostate. VP: ventral prostate. BU: bulbourethral gland. ED/EP: epididymis containing the efferent ductules. SV: seminal vesicle. n.s: not statistically significant.

or through less drastic interferences could be valuable to proper understand the molecular basis underlying the disease.

In the early 1970s, Morris Pollard showed that male rats of Wistar strain are genetically predisposed to develop prostatic adenocarcinoma at senescence [21]. More recently, we have presented evidence that aged Wistar rats are highly susceptible to the onset of histopathological alterations that mimic most of those affecting the human prostate and include both non-neoplastic and neoplastic lesions [6]. Such data entice attention to the potential use of these animals as a suitable experimental model for studying aging-related prostate disorders including PCa. However, a systematic evaluation of the changes affecting the prostates of Wistar rats as well as their incidence, is still lacking. Moreover, it is not known whether a sex steroid-induced imbalance during the window in which this rat strain becomes more susceptible to the onset (12 months) and intensification (18 months) of prostatic alterations could enhance the development of specific lesions such as adenocarcinomas. Therefore, the aim of the present study was to provide a detailed description of the broad spectrum of changes found in the prostate of Wistar rats at 18 months of age, and compared the incidence of each lesion between control and the age-matched rats treated with testosterone plus estradiol.

2. Materials and methods

2.1. Ethics statement

The experimental procedures involving animals were approved by the Ethical Committee for Animal Experimentation of the UFMG (process No. 344/2018) and conducted in accordance to the ARRIVE (Animal Research: Reporting In Vivo Experiments) guidelines.

2.2. Experimental approach

Male Wistar rats were obtained from the Central Animal House of the Universidade Federal de Minas Gerais (UFMG) and kept in a proper animal facility under controlled environmental conditions (50 ± 10% relative humidity, 22 ± 2 °C, 12 h light/ 12 h dark), with ad libitum access to water and food (Nuvilab CR1, Nuvital Nutrientes S.A, Colombo, Brazil). At 12 months of age, a group of animals (n = 16) received two Silastic capsules (2.0 cm length each) tightly filled with testosterone propionate (Cat. No. T-1875, Sigma-Andrich, USA) and one of 1.0 cm length with estradiol (Cat. No. E-8515, Sigma-Andrich, USA), both hormones in powder form. These animals (referred as T + E_2-treated rats) constituted the treatment group. The hormone-containing implants were constructed from Silastic tubes (Cat. No. 508-009, 1.98 mm inner diameter, 3.18 mm outer diameter, Dow-Corning

Table 1
Microscopic alterations and their incidence in the prostate of control and T + E2-treated Wistar rats at 18 months of age.

Histopathology	Cytological aspects	Differential features (Control vs. T + E_2)	Incidence of epithelial lesions No. (%)			p value
			Entity	Control	T + E_2	
Hydropic vacuolation	Luminal cells with cytoplasmic vacuolation of presumably aqueous appearance. Nuclei often flattened and disposed toward to the periphery.	None.	VP (only)	4 (36,4)	11 (91.7)	0.0094*
Squamous metaplasia	Basal cells undergoing aberrant proliferation that confer to the glandular epithelium a squamous stratified appearance.	None.	LP (only)	3 (27.3)	5 (41.7)	0.6668
Mucinous metaplasia	Luminal cells of globet-like morphology with accumulated mucinous materials in their supranuclear area of the cytoplasm.	None.	VP (only)	1 (9.1)	1 (8.3)	> 0.999
Abscess	Massive inflammatory infiltrate with the predominance of granulocytes closely associated with an injured epithelium	None.	LP (only)	3 (27.3)	11 (91.7)	0.0028
Hyperplasia	Cellularity augmentation leading to epithelium unfoldings.Predominance of proliferating luminal cells with no nuclear atypia.	Epithelial unfolding is more pronounced in T + E_2.	Overall	11 (100)	12 (100)	> 0.999
			LP	11 (100)	6 (50.0)	0.0137*
			VP	10 (90.9)	11 (91.7)	> 0.999
			DP	10 (90.9)	11 (91.7)	> 0.999
			AP	10 (90.9)	12 (100)	0.4783
Simple atrophy	Predominance of luminal cells with reduced height and scant cytoplasm. Cells are often in interphase and non-associated to inflamatory infiltrate.	None.	Overall	11 (100)	12 (100)	> 0.999
			LP	7 (63.6)	12 (100)	0.0373*
			VP	10 (90.9)	8 (66.7)	0.3168
			DP	9 (81.8)	9 (75.0)	> 0.999
			AP	4 (36.4)	3 (25.0)	0.3707
Proliferative inflammatory atrophy (PIA)	Predominance of atrophic luminal cells and normal-appearing basal cells. Cells often proliferate and are neighbored by inflammatory foci.	Widespread in T + E_2 and may be found in continuity with HG-PIN.	LP (only)	4 (36,4)	11 (91.7)	0.0094*
Low grade prostatic intraepithelial neoplasia (LG-PIN)	More than two layers of cells with normal or slightly enlarged nuclei sustained by a preserved basement membrane.	Unifocal in control and multifocal in T + E_2.	Overall	10 (90.9)	12 (100)	0.4783
			LP	9 (81.8)	12 (100)	0.4545
			VP	8 (72.7)	10 (83.3)	0.6404
			DP	8 (72.7)	11 (91.7)	0.3168
			AP	6 (54.5)	11 (91.7)	0.0686
High grade prostatic intraepithelial neoplasia (HG-PIN)	Three or more layers of crowded cells of irregular size and often exhibiting enlarged nuclei with prominent nuclei, sustained by a preserved basement menbrane.	Unifocal and usually present tufted and cribriform architecture in control. Multifocal and mostly of flat pattern in T + E_2.	Overall	7 (63.6)	12 (100)	0.0373*
			LP	6 (54.5)	9 (75.0)	0.4003
			VP	3 (27.3)	6 (50.0)	0.4003
			DP	0	6 (50.0)	0.0137*
			AP	0	10 (83.3)	< 0.0001*
Adenocarcinoma	Predominance of crowded cells exhibiting dysplastic features and undergoing proliferation. Basal cells are often absence in nearly but not all tumors.	Mostly invasive and poorly differentiated in T + E_2.	Overall	4 (36.4)	12 (100)	0.0013*
			LP	4 (36.4)	12 (100)	0.0013*
			VP	1 (9.1)	6 (50)	0.0686
			DP	2 (18.2)	6 (50)	0.1930
			AP	0 (0.0)	1 (8.33)	> 0.999

LP: lateral prostate. VP: ventral prostate. DP: dorsal prostate. AP: anterior prostate.
* Statistically significant difference between control and treated ($p < 0.05$).

Corporation, USA) as previously described [14], and placed subcutaneously under sterile surgical conditions into the flank region of anesthetized rats (ketamine-xylazine in combination at 60 and 8 mg/kg of body weight, respectively). To ensure consistent steroid release over time, the implants were replaced at 15 months and kept until animals reached 18 months of age. Control animals ($n = 12$) received empty Silastic implants. The animals were constantly monitored for changes in food consumption and health appearance.

2.3. Sample collection and processing

After deep intraperitoneal anesthesia (87 mg ketamine/kg and 13 mg xylazine/kg), the animals were perfused through the left ventricle with Ringer's solution followed by 10% neutral buffered formalin (NBF). The ventral, dorsal, lateral, and anterior prostatic lobes were dissected, weighed, immersed for at least 24 h in the NBF fixative solution, and then processed for paraffin embedding. Immediately prior to fixation, a small fragment (~50 mg) of each prostatic lobe was snap frozen in liquid nitrogen and stored at −80 °C. Additionally, other reproductive (seminal vesicle, bulbourethral gland, testis, and epididymis) and non-reproductive (spleen, kidney, adrenal and pituitary gland) tissues were removed, weighed and processed for future studies. Paired organs were weighted together.

2.4. Hormone measurements

Plasma samples were obtained after blood collection in heparin-coated tubes through cardiac puncture and followed by centrifugation (at 800 *g* for 5 min). The concentrations of testosterone, dihydrotestosterone, and estradiol were assessed in the plasma of control and T + E_2-treated rats with commercial ELISA Kits (Cat. No. EIA-5396, EIA-5761, and EIA-1559, DRG Instruments GmbH, DE). The assays were performed in duplicate and followed the manufacturer's instructions.

2.5. Stereology and histopathological assessment

Microscopic alterations between groups were evaluated by using routine histology and stereological analysis. For this, NBF-fixed and paraffin-embedded fragments of the prostates were sectioned at 5 μm, stained with hematoxylin and eosin (HE) or periodic acid-Schiff (PAS), and then scanned in a digital pathology system (Panoramic MIDI II, 3DHISTECH, HU). In addition, cryosections of 12 μm thickness from ventral prostates embedded in OCT compound (Sakura Finetek, USA) were stained with oil red to detect lipid-rich contents.

The relative proportion of each compartment of the gland was determined through stereological assessment. For the measurement, the

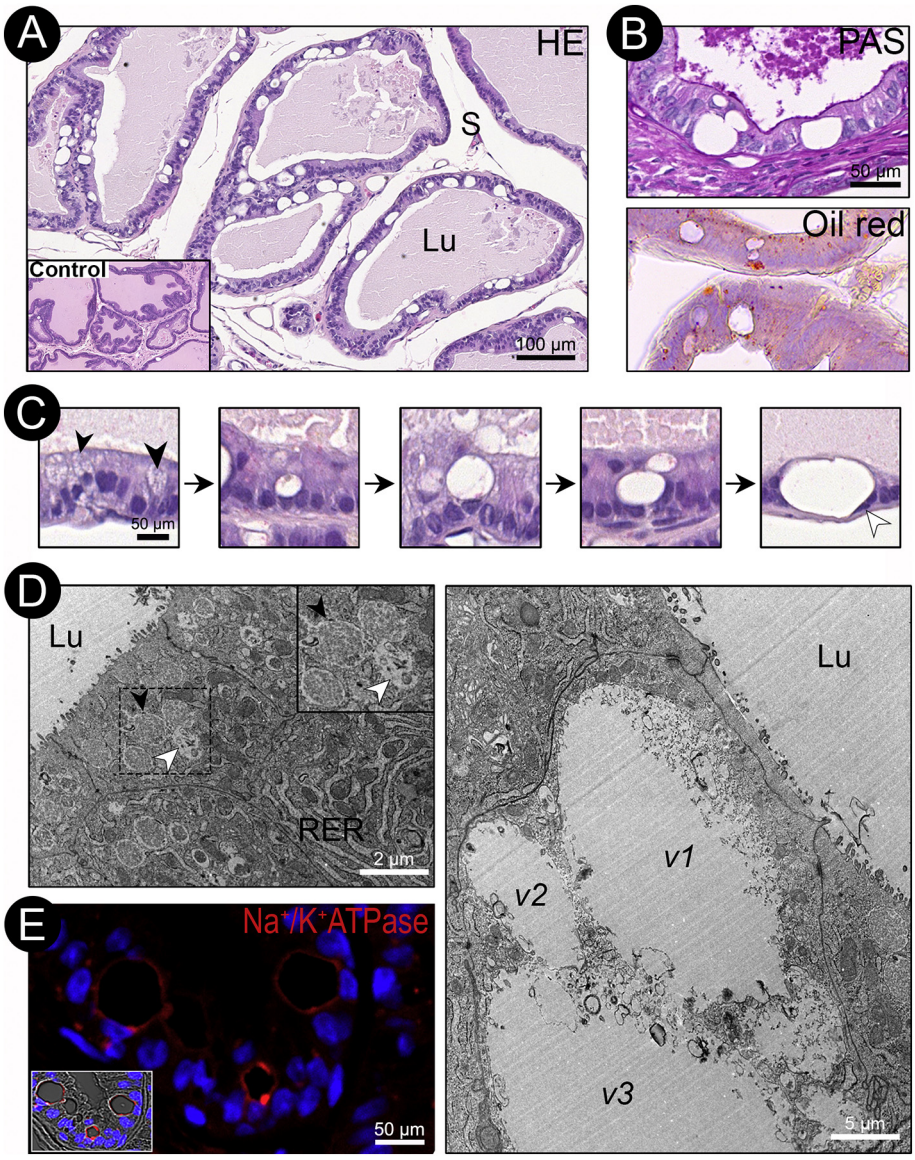

Fig. 2. Hydropic vacuolation in the ventral prostate epithelium of T + E_2-treated Wistar rats. (A) Panoramic view of the ventral prostate epithelium highlighting numerous unstained dilated vacuoles. Insert represents few epithelial vacuolation observed in the control group. (B) PAS and oil red staining showing absence of positive content inside the vacuoles. (C) Cytoplasmic vacuoles in the initial (black arrowhead), intermediate and final (white arrowhead) stages of formation. (D and D′) Ultrastructure of vacuolated epithelial cells. In the supranuclear region, rough endoplasmic reticulum cisternae (RER) and numerous secretory vesicles (black arrowhead) were seen close to small spaces containing residual material that appears to be the initial stage of vacuolation (white arrowhead). As the vacuolation advances, the vacuoles become dilated and merge with each other, as shown in v1, v2, and v3. (E) Confocal microscopy image showing NA+/K+-ATPase expression (red) in the vacuole surface. Cell nucleus was labeled with DAPI (blue). Insert represents an overlap of the image with bright field. Lu: lumen. S: stroma. (For interpretation of the references to color in this figure legend, the reader is referred to the web version of this article.)

prostate compartments were subdivided into epithelium (normal or altered), lumen (with secretion or having sloughed and/or inflammatory cells), and stroma (fibers and connective tissue cells, peri-alveolar smooth muscle layer, blood vessels, and inflammatory foci). For all animals, 10 images were randomly taken (at 40× magnification) from each prostatic lobe and the proportion of compartments was determined by counting the coincident points in a graticulate system with a total of 135 points. The results were expressed as the percentage per constituent.

The histopathological alterations observed in the prostate of control and treated rats were described based on previous investigations [22,23]. In this approach, each prostatic lobe was fragmented into 2 to 4 parts, and at least 8 different sections (stained with HE or PAS) from each fragment were evaluated. The tissue sections were scored for the presence of lesions that include epithelial vacuolation, metaplasia, hyperplasia, atrophy, prostatic intraepithelial neoplasia, and adenocarcinoma. The results were expressed as the incidence of animals affected by each lesion.

2.6. Immunohistochemistry and immunofluorescence

We performed immunohistochemical and immunofluorescence assays to evaluate the epithelial cell type predominant in each prostatic lesion and the expression status of markers implicated with tissue homeostasis and tumorigenesis. For this purpose, tissue sections of NBF-fixed and paraffin-embedded prostate fragments were obtained after serial sectioning at 4 µm and submitted to the protocol previously established [24]. The panel of antibodies used herein is specified in Table S1 and includes markers of basal cells (CK5, CKHMW), cellular proliferation (MCM7), epithelial-mesenchymal transition (E-cadherin, N-cadherin, and Vimentin), and ion transport (NA^+/K^+-ATPase).

After mounting the slides, the immunofluorescence images were acquired using the inverted Nikon Eclipse Ti confocal microscope coupled to an A1 scanning, while those from immunohistochemistry assays were obtained in the 3DHISTECH Panoramic MIDI II slide scanner.

2.7. Transmission electron microscopy (TEM)

Fragments of approximately 1 mm^3 from the ventral prostate were fixed in 2,5% glutaraldehyde for 24 h and post-fixed in 2% osmium tetroxide and then proceeded for standard epoxy resin embedding. Digital images were acquired after examination of ultrathin sections with a Tecnai- G2-Spirit FEI/Quanta electron microscope, operating at

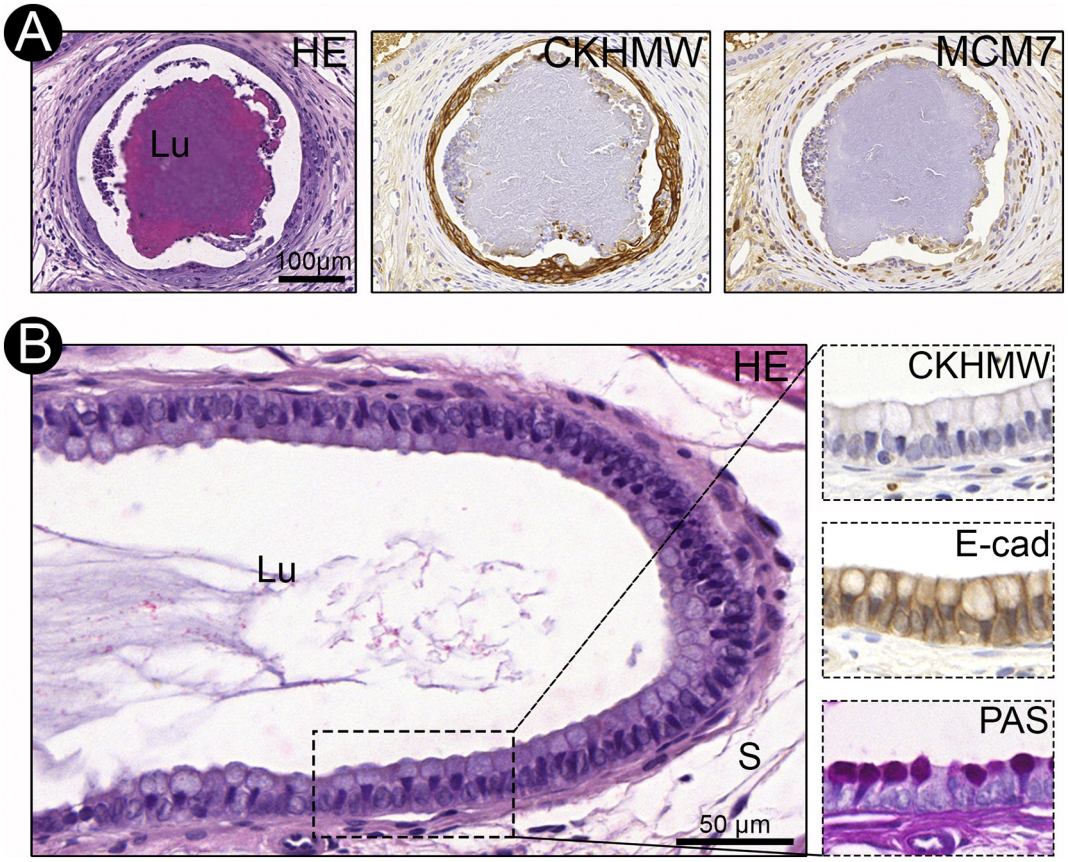

Fig. 3. Metaplastic lesions in the prostate of senile Wistar rat. (A) Lateral prostate acinus exhibiting squamous metaplasia. CKHMW and MCM7 staining were used to identify basal and proliferating cells, respectively. (B) Ventral prostate epithelium undergoing mucinous metaplasia characterized by atypical cells showing a strong PAS positive content and surface well delimited by E-cadherin staining. The figures were taken from control animals. Lu: lumen. S: stroma.

120 kV.

2.8. Protein extraction and Western blotting

Frozen tissues (50 mg) from the ventral and lateral prostates were macerated in dry ice and then solubilized in 150 μL of urea buffer (8 M urea, 20 mM Tris-HCl pH 7.5, 0.5 mM EDTA pH 8.0, 5% protease inhibitors) using a rotor-stator homogenizer. After centrifugation (10 min, 14.000 g, 4 °C), the supernatant fraction was collected from each sample (n = 5 per group) and the protein content was determined by spectrophotometer (NanoDrop 1000, Thermo Scientific, USA).

Western blotting assays were used to evaluate changes in total protein levels of E-cadherin, β-catenin, N-cadherin, and vimentin, recognized markers implicated with epithelial-mesenchymal transition. Initially, 40 μg protein was loaded onto an 8% SDS-PAGE, separated by electrophoresis and then transferred to nitrocellulose membranes. After blocking with 5% BSA/TBST solution, the membranes were incubated *overnight* at 4 °C with the primary antibodies diluted in blocking solution. The immunoreaction was visualized after exposure for 1 h at room temperature to horseradish peroxidase (HRP)-conjugated secondary antibody followed by ECL detection (Cat. No. 20-500-500, Biological Industries, USA). Protein levels were compared between groups by evaluating the signal intensity of target protein bands normalized to that of β-actin (internal control) [25].

2.9. Statistical analyses

Statistical analyses were carried out by using the GraphPad Prism 7 analytical tools. After assessment of normality with the D'Agostino-Pearson test, quantitative variables from control and T + E_2-treated rats were compared by two-tailed unpaired *t*-test or the Mann-Whitney test, when appropriate. The data were presented as mean ± standard error of the mean (SEM). As a categorical data, the incidence of prostatic lesions between groups was presented as frequency and analyzed by Fisher's exact test. Differences were considered significant when obtaining a $p < 0.05$.

3. Results

3.1. Macroscopic and microscopic changes in the rat prostates in parallel to increased levels of testosterone and estradiol

To drive histopathological alterations in the prostate, intact 12-month old Wistar rats were treated for 6 months with Silastic implants containing testosterone plus estradiol. Control animals received empty implants (Fig. 1A). The survival analysis showed that although 5 out of 28 animals died over the experimental course (1/12 controls; 4/16 treated), the long-term hormone exposure was tolerated by the majority (75%) of the animals (Fig. 1B). The treated rats terminated the experiment period in a good health appearance similar to controls, even after undergoing a progressive weight loss of 82 ± 13 g (Fig. 1C). As expected by the hormonal treatment, the concentration of testosterone, dihydrotestosterone, and estradiol was significantly higher in the plasma of T + E_2-treated rats (Fig. 1E).

The treatment induced notorious macroscopic modifications in regard to sizes and appearance of the prostatic complex, especially the lateral prostate, which presented firm and dense bands of yellow-brown tissue (Fig. 1D). In addition, the weight of all the prostate lobes was significantly higher in T + E_2-treated than in control animals (Fig. 1F). The treatment schedule appeared to play primary adverse effects

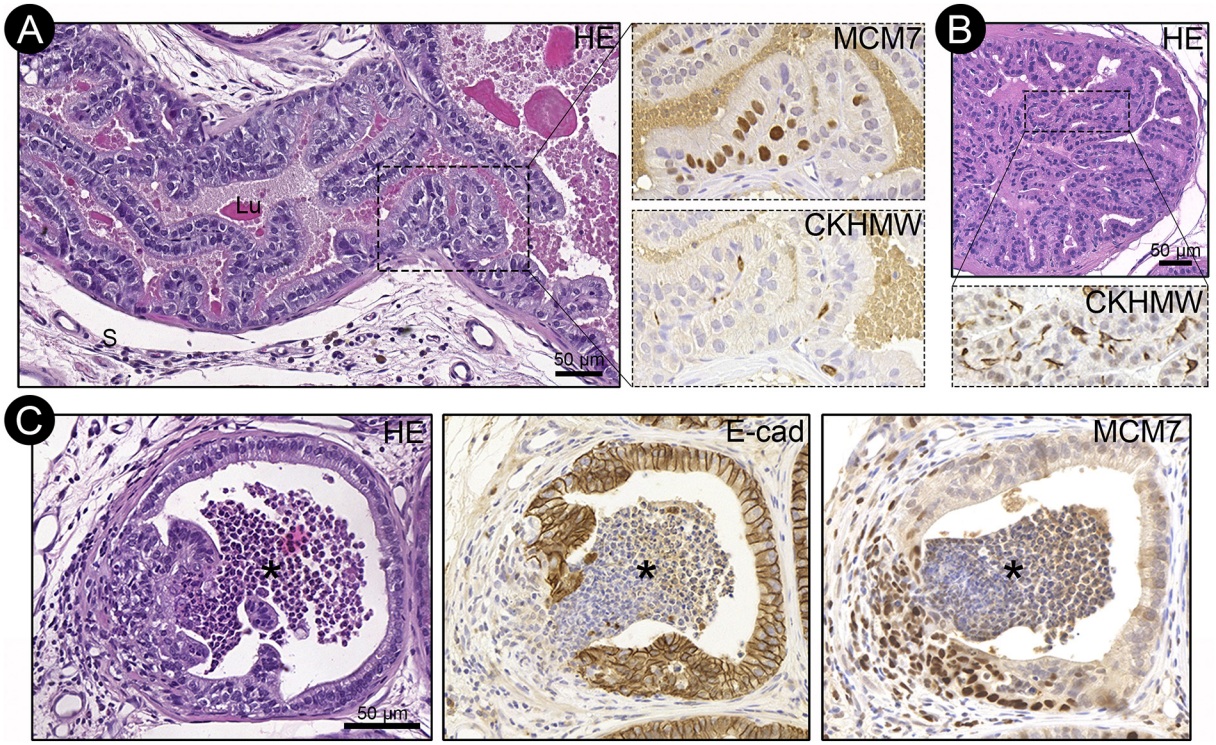

Fig. 4. Hyperplasia and abscess in the prostate of senile Wistar rats. (A) Hyperplastic epithelium from the lateral prostate of T + E_2-treated animals showing cellularity augmentation and projecting moderate unfolding toward the lumen. Hyperplastic foci were actively proliferating as they presented immunoreactivity for MCM7, and showed predominance of luminal cells (CKHMW negative). (B) Occasionally in the treatment group, the anterior prostate also exhibited areas of basal cell hyperplasia, as detected by the high number of CKHMW-positive cells. (C) Prostate abscess in the lateral prostate of a T + E_2-treated rat. This lesion shows focal areas with vast infiltrate of polymorphonuclear cells (*) reaching the lumen and rupture of the associated epithelium, as indicated by the absence of epithelial cells expressing E-cadherin. MCM7-positive proliferating cells were observed in the lesioned epithelium. Lu: lumen. S: stroma.

mainly on the organs most responsive to steroid hormones, since differences in weights and gross morphology were also observed for seminal vesicle, testis, epididymis, and pituitary gland, but not for other organs such as kidney, adrenal gland, and spleen (Fig. 1D, F and Fig. S1A). As previously portrayed in this type of chronic intervention (13–15), testicular atrophy and pituitary adenomas were commonly found in T + E_2-treated rats (Fig. S1A, B).

At the microscopic level, significant modifications were detected in the prostatic tissue after treatment. As evidenced by stereological analysis (Table S2), such modifications were more prominent in the lateral followed by the ventral, dorsal and anterior prostates, and included: (i) marked decrease of acini and ductus with normal features associated with higher prevalence of epithelial sites exhibiting histopathological alterations; (ii) increased density of blood vessels and inflammatory foci in the stroma; (iii) prevalence of leukocytes and sloughed epithelial cells into the lumen; and (iv) lobe-specific variation in the thickness of perialveolar smooth muscle layer.

3.2. Chronic combination of testosterone plus estradiol enhances the incidence of benign, pre-malignant and cancerous lesions in the prostate epithelium

A broad spectrum of lesions was observed in the rat prostate at 18 months of age, in both control and treatment group; however, the changes observed in control animals were punctual and restricted to few epithelial areas randomly distributed alongside acini and ducts with unaltered morphology, whereas a large extent of the prostatic epithelium of T + E_2-treated animals presented some histopathological alteration (for an overview, see Fig. S2). The changes included benign, pre-malignant and tumor lesions, whose incidence and extent varied according to experimental group and prostate lobe (Table 1). For a better understanding, herein we provide a detailed comparative description of each epithelial lesion that arose in the prostates of control and treated rats.

3.2.1. Hydropic vacuolation

Some epithelial cells presenting cytoplasmic vacuoles were observed primarily in the ventral prostate epithelium. They likely correspond to atypical luminal cells, based on the absence of CK5 and CKHMW staining (data not shown). Notably, the treatment with T + E_2 functioned as a potent inducer of epithelial vacuolation, since the number of animals presenting vacuolated epithelial cells was significantly higher in the treatment group (4/11 controls vs. 11/12 treated, $p = 0.0009$, Table 1). The vacuoles were often larger and occupied a space of the epithelium that could fit two or more luminal cells (Fig. 2A and C). After careful histological and ultrastructural analysis, we found that the vacuolation appeared to involve a progressive ballooning of vesicles in the supranuclear cytoplasm which coalesced to form dilated vacuoles. As the vacuoles increase in size, they merge with each other and usually force the nucleus and residual cytoplasm toward the cell margin (Fig. 2C, D). Thus, it was possible to see within the same epithelial area, cells exhibiting visible cytoplasmic vacuoles at different stages of formation (Fig. 2C). Noteworthy, the vacuoles neither presented electron-dense content nor were stained for HE, PAS or oil red, thereby being structures of presumably aqueous character (Fig. 2B–D). This hypothesis of hydropic vacuolation was corroborated by the intense expression of NA^+/K^+-ATPase located especially in the vacuole surface (Fig. 2E), which is suggestive of hydrolytic imbalance.

3.2.2. Squamous metaplasia

The prostate of aged Wistar rats also displayed areas of squamous metaplasia, a benign lesion in which the aberrant proliferation of basal cells conferred to the prostatic epithelium a squamous stratified appearance (Fig. 3A). The accurate identification of this lesion was

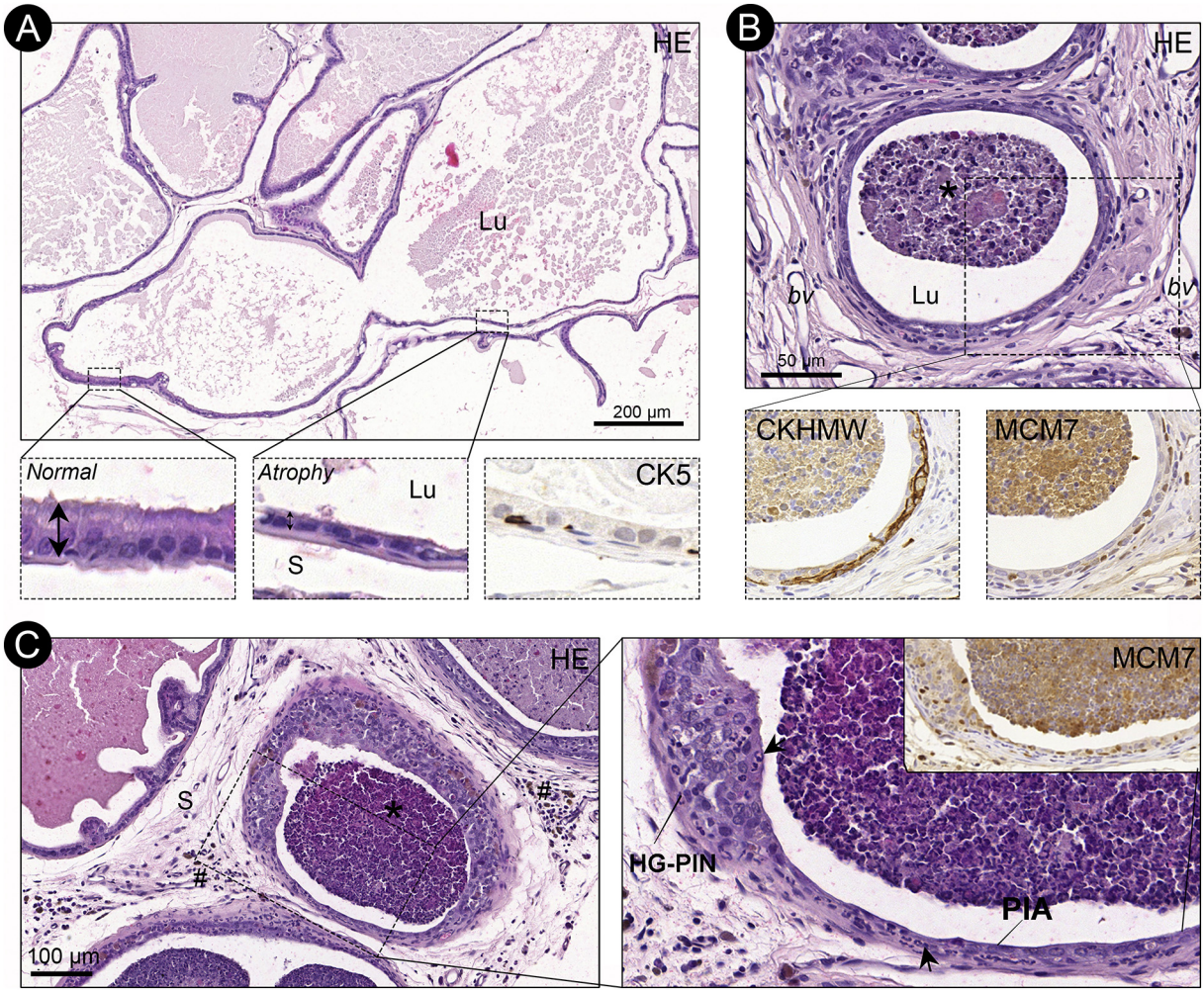

Fig. 5. Atrophic lesions in the prostates of senile Wistar rats. (A) Representative ventral prostate of a control animal exhibiting atrophic luminal cells (CK5 negative). Double arrow highlights the difference in height between normal-appearing and atrophic cells. (B) Atrophic lesion in the lateral prostate of a T + E_2-treated rat showing features of PIA, in which the lesioned acini are actively proliferating (MCM7 positive) and occur in a tight association with inflammatory cells that surround the acini (#) and/or localize within the epithelium (arrowheads) and lumen (*). PIA exhibited a characteristic enrichment of basal cells (CKHMW positive). (C) Some PIA lesions occurred in continuity with HG-PIN. Lu: lumen. S: stroma. bv: blood vessel. PIA: proliferative inflammatory atrophy. HG-PIN: high grade prostatic intraepithelial neoplasia.

performed by using the routine histology in association with immunohistochemical staining for recognized markers of basal cells (CKHMW) and cellular proliferation (MCM7). Acini exhibiting squamous metaplasia were observed only in the lateral prostate. The number of animals having this lesion was quite similar between groups (3/11 control vs. 5/12 treated, p = 0.6668, Table 1).

3.2.3. Mucinous metaplasia

It was characterized by cells displaying goblet-like morphology and that accumulate mucinous materials (strongly positive for PAS) in their supranuclear cytoplasm (Fig. 3B). Based on the absence of CKHMW staining, the mucinous cells likely correspond to luminal cells (Fig. 3B). These metaplastic cells occurred scattered or forming small groups in the ventral prostate epithelium and affected only one animal of each group (Table 1). The atypical cells presented a precise delimitation as indicated by the staining pattern of the membrane-anchored protein E-cadherin (Fig. 3B).

3.2.4. Hyperplasia

Present in the prostate of all control and treated rats (Table 1), hyperplasia was identified by a glandular epithelium showing cellularity augmentation and immunopositivity for MCM7 (Fig. 4A). In the control group, hyperplastic acini were punctual and showed slight to moderate unfolding toward the lumen. Conversely, numerous hyperplastic sites projecting moderate to extensive epithelial unfolding that often occupied a great area of the lumen were found within the prostates of T + E_2-treated rats (Fig. 4A). In most cases, hyperplastic cells corresponded to luminal cells as they did not express CKHMW, except in the anterior prostate of some treated rats, where basal cell hyperplasia was also observed (Fig. 4B).

3.2.5. Abscess

Focal areas presenting a vast inflammatory infiltrate with predominance of polymorphonuclear cells closely associated with a lesioned epithelium were observed in the prostate of few controls but almost all T + E_2-treated rats (3/11 controls vs. 11/12 treated, p = 0.0028, Table 1) (Fig. 4C). These areas were found only in the lateral prostate and correspond to abscesses, in which the acute inflammatory response leads to injury of the associated epithelium. Such tissue damage was easily observed since the epithelium in contact with the inflammatory infiltrate underwent a discontinuity, as confirmed histologically and by the absence of epithelial cells expressing E-cadherin specifically at this site. In addition, it was common to detect MCM7-positive epithelial cells in the lesioned epithelium (Fig. 4C).

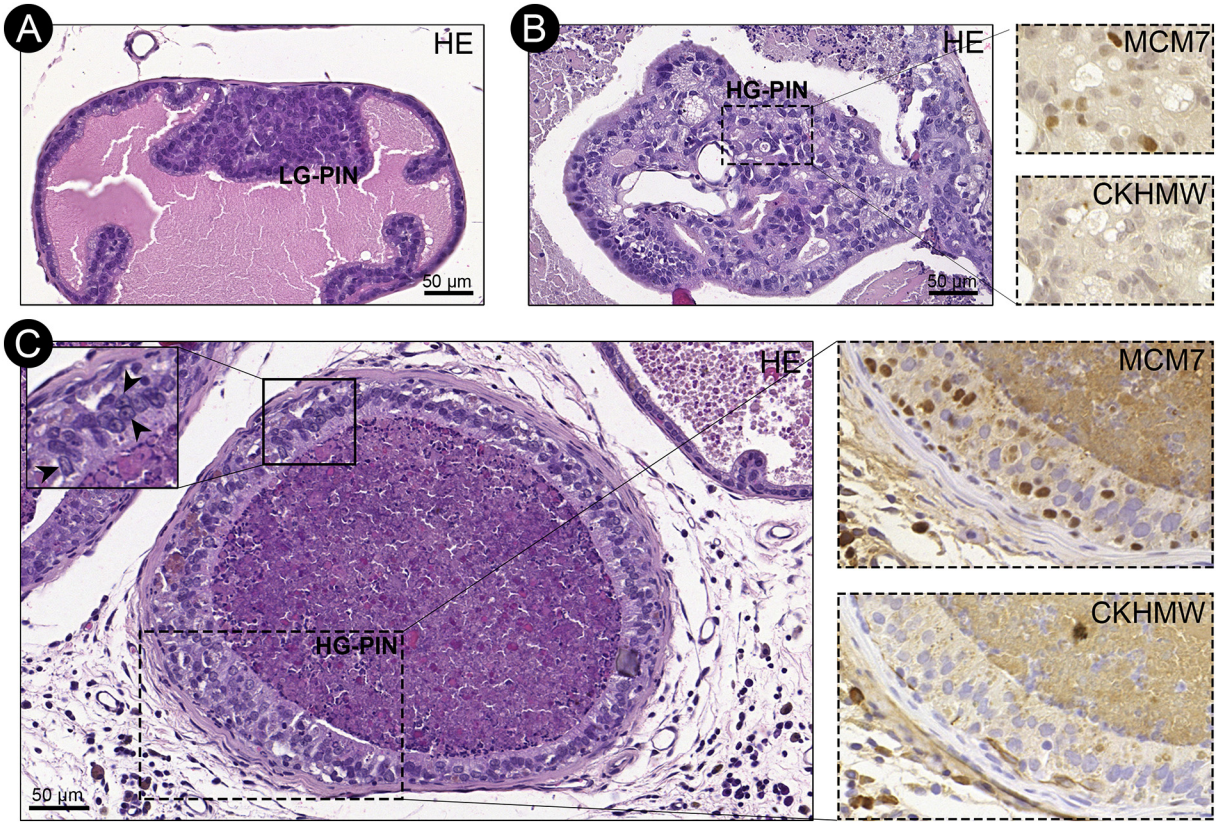

Fig. 6. Prostatic intraepithelial neoplasia in the prostates of senile Wistar rats. (A) Representative HE staining from the lateral prostate of a control animal presenting a LG-PIN. (B) Ventral prostate of a control rat showing a HG-PIN with cribriform pattern and some proliferative MCM7-positive cells. (C) HG-PIN from the lateral prostate after T + E_2 treatment. Layers of epithelial cells with enlarged nuclei and prominent nucleoli (arrowheads), many of them in proliferation, are arranged in a flat architecture. LG-PIN: low-grade prostatic intraepithelial neoplasia. HG-PIN: high-grade prostatic intraepithelial neoplasia.

3.2.6. Atrophies

Another frequently observed prostatic lesion was epithelial atrophy, in which ducts and acini were lined by a cubic to squamous epithelium composed of luminal cells with reduced height and scant cytoplasm, as well as normal-appearing basal cells (Fig. 5). Regardless of experimental group, epithelia undergoing atrophy were observed in the prostate of all animals (Table 1). Despite the majority of atrophies were histologically correspondent to focal simple atrophies, this group of lesions showed to be heterogeneous among prostate lobes and even within the same gland. Accordingly, in the ventral prostate, which was the lobe with the highest extent of atrophic lesions, it was possible to observe glands either partially or completely lined by an atrophic epithelium (Fig. 5A). Particularly in the lateral prostate, glandular atrophy often corresponded to proliferative inflammatory atrophy (PIA), as such lesions were actively proliferative and occurred in a tight association with inflammatory cells surrounding the acini and/or located within the epithelium and lumen (Fig. 5B and C). Differently from simple atrophy, PIA also exhibited a characteristic enrichment of basal cells that usually were arranged beneath or alongside the atrophic luminal cells (Fig. 5B). Importantly, the chronic treatment with T + E_2 potentiated the development of PIA, as these lesions were found widespread in the lateral prostate of almost all treated rats (11/12, ~92%). It is noteworthy that PIA was often found in continuity with prostatic intraepithelial neoplasia, within the same acini (Fig. 5C). In contrast, limited sites containing PIA were found in the lateral prostate epithelium of control animals (36%, 4/11) (Table 1).

3.2.7. Prostatic intraepithelial neoplasia (PIN)

Lesioned areas compatible with PIN were defined through the observation of intraepithelial stratification sustaining luminal cells of varying sizes and nuclear appearance, and a preserved basement membrane (Fig. 6). PIN lesions were classified as low (LG-PIN) or high grade (HG-PIN) according to the predominant morphological features of epithelial cells. LG-PIN was characterized by more than two layers of cells displaying normal or slightly enlarged nuclei with prominent nucleoli (Fig. 6A), whereas the HG-PIN showed three or more layers of crowded cells of irregular size often exhibiting enlarged nuclei with prominent nucleoli and immunopositivity for MCM7 (Fig. 6B and C). Regardless of experimental group, both PIN lesions affected mainly the glands of the lateral prostate. However, LG-PIN and HG-PIN were unifocal within the glands of control animals, since they uniquely affected isolated sites scattered throughout the normal epithelium, whereas in the treatment group, the lesions could be seen in multiple epithelial sites. Noteworthy, as presented in Table 1, the number of animals carrying HG-PIN was significantly higher in the treatment group (7/11 controls vs. 12/12 treated, $p = 0.0373$). The same did not occur for LG-PIN, since this lesion was commonly present in almost all animals (10/11 controls vs. 12/12 treated, $p = 0.4783$). Moreover, the architectural patterns of HG-PIN varied according to the experimental group, as the lesion frequently assumed a tufted or cribriform pattern in the lateral and ventral prostate of controls (Fig. 6A and B), respectively, and a flatter architecture in the prostatic lobes of T + E_2-treated rats (Fig. 6C). It is important to emphasize that, because inflammatory foci were frequently observed close to or associated with HG-PIN in the treatment group (Fig. 5C and 6C), this proliferative lesion could be misidentified as the reactive hyperplasia, a non-neoplastic/inflammatory lesion of the prostate [22,23]. However, the diagnostic features to discriminate these lesions rule out the possibility of reactive hyperplasia [23], as HG-PIN presented many atypical cells and the associated inflammatory infiltrate was not suppurative.

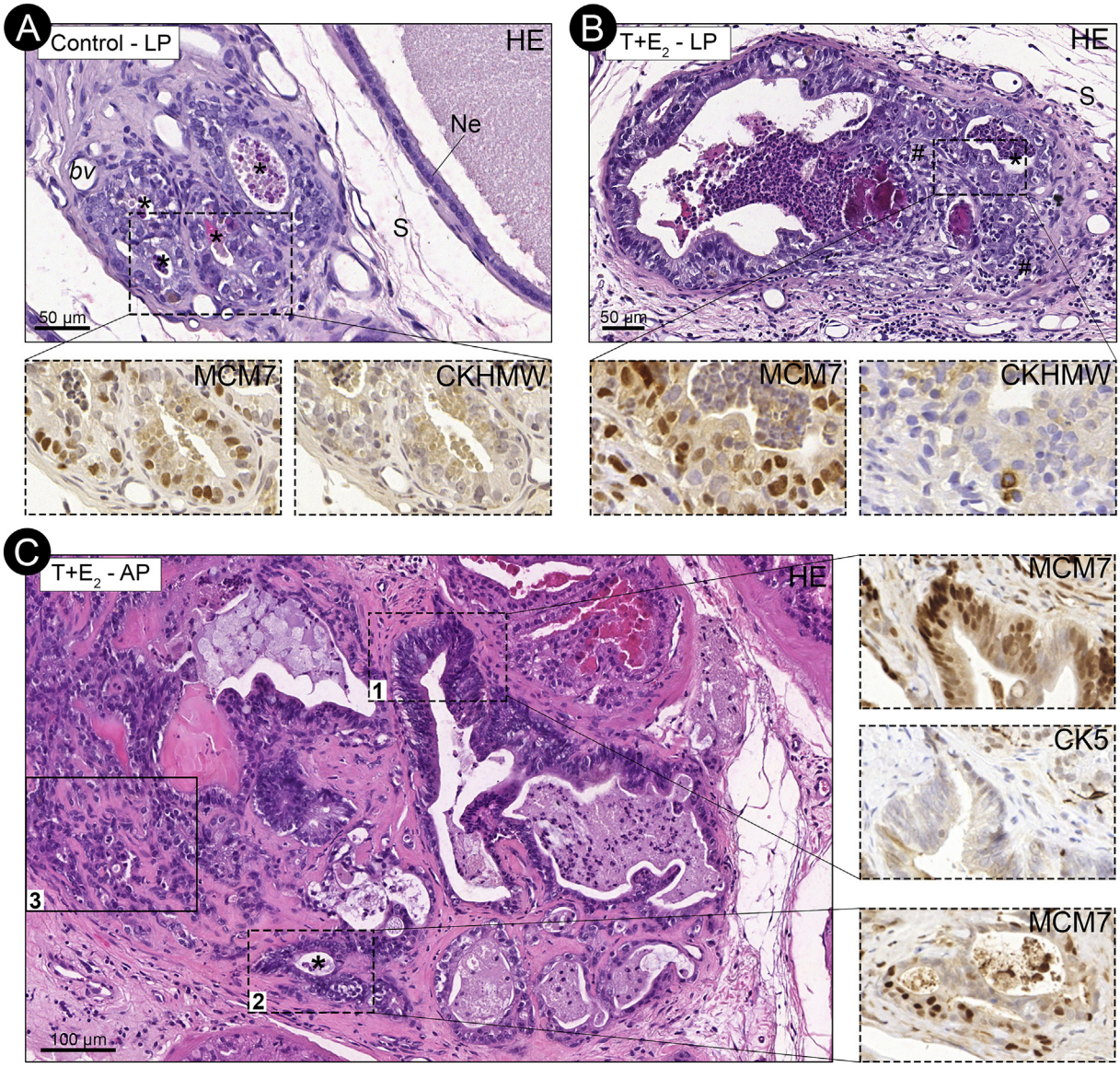

Fig. 7. Adenocarcinoma in the prostates of senile Wistar rats. (A) Ventral prostate of a control animal showing malignant cells forming microacini. (B) Invasive adenocarcinoma in the lateral prostate of a T + E_2-treated rat. Microacini arrangement is present, as well as malignant cells diffused through the stroma in close association with inflammatory infiltrate. (C) Treated anterior prostate in panoramic view, showing different stages of adenocarcinoma: 1 - adenocarcinoma in situ, with dysplastic cells; 2 - microacini formations; 3 - poorly differentiated invasive adenocarcinoma spread through the stroma. Regardless of experimental group, the majority of malignant sites showed high proliferative activity (MCM7-positive) and exhibited predominance of CKHMW-negative cells. S: stroma. Ne: normal epithelium. bv: blood vessels. *: indicates microacini arrangement.

3.2.8. Adenocarcinoma

The occurrence of the premalignant lesions HG-PIN and PIA raised the possibility of detecting tumors in the rat prostate at 18 months of age. After a systematic screening of several histological slides from each prostate lobe, we were able to detect lesions histologically-compatible with adenocarcinomas in the prostates of both groups analyzed. The malignant sites had an abnormal growth pattern with the predominance of crowded, basophilic, dysplastic-appearing cells. The majority of tumors were actively proliferative and did not present positive staining for the basal cell markers CKHMW and CK5 in the epithelium (Fig. 7). One exception was observed in a tumor growing in an intraductal pattern within the lateral prostate of a control animal, where the retention of the basal cell layer, characteristic in this type of adenocarcinoma, was observed (Fig. S3). However, it is important to note that the effects of long-term hormone exposure for inducing prostatic adenocarcinoma surpassed those of physiological aging. Indeed, while a modest incidence of malignant lesions (4/11, 36%) was computed in the control group, 100% (12/12) of T + E_2-treated rats had adenocarcinomas in their prostates. Moreover, unlike the control group in which both in situ and invasive adenocarcinomas were observed, the majority of malignant sites found in the treated animals corresponded to invasive adenocarcinomas arranged in a microacinar architecture or entirely widespread in the stroma (Fig. 7). In consonance with the observation of premalignant lesions, in both control and treated rats, the lateral lobe was the major target for tumors, followed by the dorsal, ventral, and anterior prostates (Table 1).

3.3. The effects of T + E_2 treatment on the rat prostate include induction of epithelial-mesenchymal transition

The epithelial-mesenchymal transition (EMT) is a cellular transdifferentiation program highly implicated with the prostate tumorigenesis, and both androgens and estrogens can modulate EMT-inducing signals [26–28]. Thus, in this study, we sought to investigate whether the

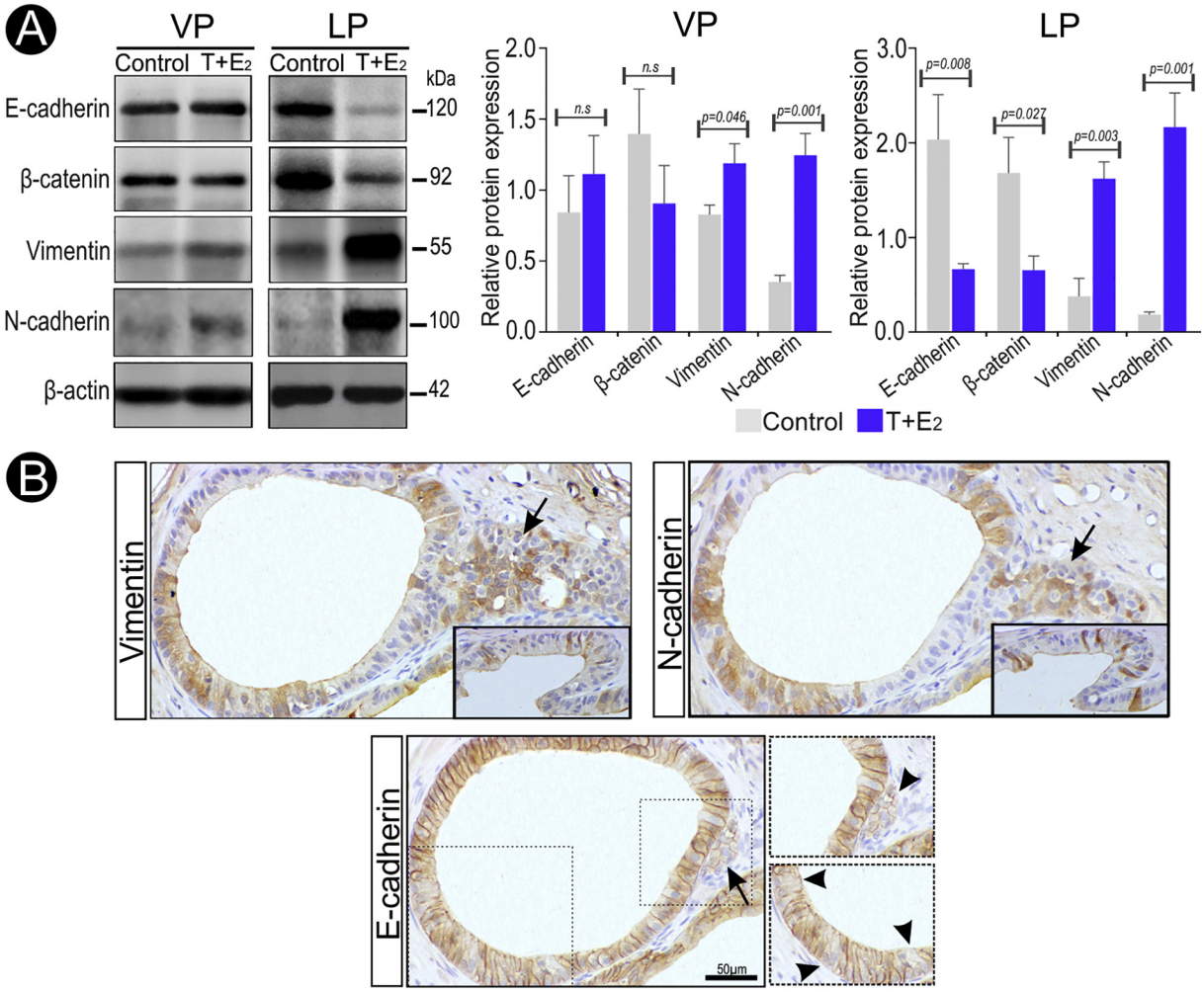

Fig. 8. The effects of T + E_2 treatment on the rat prostate include induction of epithelial-mesenchymal transition. (A) Representative images of Western blotting assays followed by densitometric quantification of immunoreactive bands correspondent to EMT-associated proteins. Note that the changes were more pronounced in the lateral than ventral prostate (B) In line with the main changes observed in total protein extracts, numerous prostate epithelial cells of T + E_2-treated rats became positive for vimentin and N-cadherin while showing flaw in the expression of E-cadherin (arrowheads). Such epithelial cells occurred restricted to areas with altered morphology and portraying lesions such as invasive adenocarcinoma (arrows). Lower inserts highlight the presence of immunoreactive epithelial cells displaying elongated morphology. Pictures were taken from the lateral prostate. VP: ventral prostate. LP: lateral prostate.

enhanced malignant transformation of the prostate epithelium following chronic exposure to T + E_2, such as that observed in the ventral and especially in the lateral prostate, might be associated with changes indicative of EMT.

Western blotting results showed that, while the total level of the cell-cell adhesion molecules E-cadherin and β-catenin remained unchanged in the ventral prostate, their expressions were drastically reduced in the lateral prostate of T + E_2-treated rats (Fig. 8A). On the other hand, the treatment upregulated the expression of vimentin and N-cadherin in the ventral and especially in the lateral prostate (Fig. 8A). Accordingly, in the lateral prostate of treated rats, epithelial cells frequently expressed vimentin and N-cadherin, both mesenchymal proteins that upon physiological conditions are absent in the epithelium. These epithelial cells eventually presented an elongated mesenchymal-like morphology and were found restricted to lesioned areas including HG-PIN and invasive adenocarcinoma, which often showed flaws in expressing epithelial markers such as E-cadherin (Fig. 8B). Altogether, the chronic combination of testosterone plus estradiol affects the expression of epithelial and mesenchymal proteins characteristic of EMT phenotype in a lobe-specific manner. This finding goes in line with the higher incidence of tumors and the pre-malignant lesions HG-PIN and PIA in the lateral prostate of T + E_2 rats (Table 1).

4. Discussion

The present study explored two relevant issues for prostate health: aging and the influence of androgen and estrogen balance. By using the Wistar rat as an experimental model, we showed that at advanced ages, the prostate is targeted by histopathological alterations including benign, premalignant, and malignant lesions, which resemble the aging human prostate in many respects. Strikingly, the incidence of most prostatic alterations including precancerous lesions and adenocarcinomas increased expressively after treatment of middle-aged rats with testosterone plus estradiol, an enhancement that was associated with molecular changes hallmark of epithelial-mesenchymal transition (EMT).

The results presented herein, as well as those from previous investigations [6,21,29,30], demonstrated that aged Wistar rats are highly susceptible to the arising of prostate lesions. Even in the control group, punctual areas exhibiting proliferative, atrophic, metaplastic and inflammatory lesions were observed in the prostate. Since the control animals received empty hormone implants, the changes observed in this group are assumed to be spontaneous and resultant from the aging process. It is important to highlight that, besides the non-neoplastic lesions found in control rats, around 36% of them developed

malignant prostatic tumors. Such tumor rate is close to the 26% previously found for this rat strain at advanced ages [29] and far away exceeds those observed in senescent mouse (< 1%) and hamster (2%) [[31],32]. It also exceeds those reported for other rat strains, such as NBL (0.45%, over 13 months old [9]), F344 (3,4%, at 24 months [33]), Copenhagen (10%, at 36 months [3]), and AXC rats (17%, at 34 to 37 months [17]). Only the ACI/Seg rats aged 33 months and beyond presented a higher incidence of PCa than the presently found, which was reported to reach up to 80% [3,34]. These data suggest that the use of Wistar rats provide advantages over other experimental animals, since they present a modest incidence of spontaneous tumors within a shorter period of time (18 months). Additionally, similar to that commonly found in elderly men, malignant tumors arising in the prostate of aged Wistar rats corresponded to adenocarcinomas, as reported here and by others [21,29].

Besides the animal's age and strain, the detection of naturally occurring PCa is also dependent on the success in sampling the target area. In this study, malignant lesions occurred in punctual areas surrounded by normal-appearing acini and ducts and were not present in the majority of histological slides. Such difficulty in sampling the proper site of prostate lesions had been noticed by others [18,33]. Furthermore, doubts concerning histological discrimination between the precancerous lesion HG-PIN and non-invasive adenocarcinoma have made the diagnosis of PCa and the reliable estimation of its incidence challenging. In this regard, we argue that our approach succeeded in detecting a tumor rate of 36% in untreated Wistar rats due to an exhaustive evaluation of several histological slides taken from different regions of the prostate, in association with key immunohistochemical assays. This fact may explain why we hinted at the possibility but did not confirm previously the occurrence of prostatic adenocarcinomas in aged Wistar rats at that time [6].

The treatment with T + E_2 provided an environment conducive to a greater development of some specific lesions in Wistar rats. One of them was prostatic adenocarcinoma, whose incidence rose from 36% to 100% after the treatment. Such an impressive increment in tumor rate was accompanied by an enhancement of HG-PIN and PIA, recognized precursor lesions of PCa [35]. This data suggests that, like the human disease, PCa development in Wistar rat appears to result from a multistep process involving the onset and progression of premalignant lesions. Intriguingly, it has been thought that a prolonged period of treatment with T + E_2 is needed to effectively induce PCa in rats. For instance, Drago (1984) [12] showed that the incidence of microscopic carcinomas in the prostate of NBL rats jumped from 3.3% to 88% when the treatment period went from 3 to 18 months or longer. Similarly, Bosland et al. (1995) [14] demonstrated that the significant induction of PCa was achieved in NBL and Sprague-Dawley rats after treatment with T + E_2 for approximately 12 months. Conversely, we succeeded in inducing PCa in 100% of middle-aged rats followed by 6 months of treatment. Therefore, it is reasonable to infer that such a high inducement of PCa was not entirely due to the prolonged duration of treatment, but rather the time-life period in which the changes in androgen and estrogen levels occurs. In this line, by evaluating Wistar rats from 3 to 24 months of age, we have recently shown that changes in the circulating and intraprostatic ratio of androgen:estrogen begin at 12 months and intensify at 18 months [6], the time window at which we hereupon performed the treatment.

Recent studies on prostate cells have addressed that key factors involved with EMT can be modulated by androgens and estrogens [22–27,36]. By evaluating the expression of the EMT hallmark proteins E-cadherin, N-cadherin, β-catenin, and vimentin, herein we presented evidence that EMT might be linked to the greater development of precancerous lesions and adenocarcinomas observed after T + E_2 treatment. The EMT-associated modifications were more pronounced in the lateral prostate, which was the prostatic lobe that exhibited the highest incidence of histopathological alterations of premalignant and malignant nature. These data are in agreement with other studies showing that EMT is a putative mechanism of carcinogenesis and tumor progression in the prostate gland [26,27], although they do not exclude the possibility of androgens and estrogens may also be acting via other mechanisms to induce the adverse effects presently observed, as such hormones are well known to have a broad action in the prostatic tissue.

It has been shown that both androgen and estrogen play a role in recruiting inflammatory cells to the prostate [37–39]. This fact entices special attention because it was notorious the presence of neutrophils and mononuclear inflammatory cells in the stroma and within the lumen and epithelium of the prostate of all T + E_2-treated rats, which is indicative of active prostatitis [22]. Moreover, the treatment expressively increased the occurrence of prostate abscess. Although this lesion is often caused by bacterial infections [40], the animals of both groups were maintained under the same environmental conditions and without documentable infections. Thus, the increased frequency of abscesses in the treatment group is likely resulting from a complication of prostatitis. Importantly, besides being the lobe more affected by inflammatory disorders, the lateral prostate was the major site where premalignant lesions and adenocarcinomas arose. Although it was not the focus of the current study, the proper identification of leukocyte subsets as well as their products could be valuable to better understand the crosstalk between inflammation and the enhancement of malignancies in the prostate of T + E_2-treated rats.

Furthermore, the hormonal intervention functioned as a potent inducer of epithelial vacuolation. Vacuolated cells were primarily observed in the ventral prostate epithelium, which has been noticed as the prostatic lobe most susceptible to this alteration [6,18,41,42]. If on the one hand this data highlights the influence of sex steroids triggering vacuolation, on the other there is not yet a consensual term to designate this morphological phenomenon in the prostate [6,18,22,41,42]. Additionally, little is known about the nature of the vacuoles. In the present investigation, we used a combination of light, confocal and transmission electron microscopy to better characterize this alteration. The ultrastructural changes in association with the absence of lipid or glycoprotein rich content within the vacuole led us to propose the hydropic degeneration as the most plausible cause of vacuolation. In line with this piece of evidence, hydropic degeneration followed by vacuolation was also observed in the human prostate epithelium after treatment with the estrogenic compound diethylstilbestrol (DES) [43]. Moreover, it was observed an intense expression of NA^+/K^+-ATPase at the vacuole surface, which can disturb the equilibrium of osmotic pressure and contribute to water inflow into the vacuole.

Given the above background, our results highlight the potential use of aged Wistar rats as a suitable model to study prostatic lesions. Besides its advantages in regard to the higher PCa incidence and shorter latency period over the pre-existent spontaneous and hormonally-induced rodent models [16,44], the proposed animal model could serve as a valuable alternative to identify preventive or therapeutic measures for the prostate gland. Accordingly, a plethora of non-neoplastic and neoplastic lesions was presently described, thereby allowing evaluating, simultaneously, whether a particular target exerts effective actions against one or more histopathological alteration. On the other hand, for researchers who aim to generate preliminary or rapid insights into prostate diseases, the in vitro assays or other animal models such as those established from more drastic conditions (e.g. genetically engineered mice) might be more attractive. Nevertheless, a plausible alternative to circumvent the relatively long period of animal aging presently proposed would be purchasing animals at an advanced age, a service already offered by some animal production facilities. Also, in this study, we did not investigate if the invasive adenocarcinomas could metastasize to other organs. Further investigations are needed to evaluate the potential use of aged Wistar rats to study the metastatic PCa.

5. Conclusion

Taken together, our results provide solid evidence that male Wistar rats may be useful as a suitable preclinical model for studying aging-related prostate disorders including PCa. This statement is based upon the observation that such rat strain nicely recapitulates the prostate carcinogenesis through the arising of benign, precancerous and malignant lesions, and above all naturally yields a modest incidence of PCa that can be increased up to 100% following exposure to testosterone plus estradiol.

Acknowledgments

Funding

This work was supported by the Conselho Nacional de Desenvolvimento Científico e Tecnológico - CNPq/Brazil (Grant and research fellowship to C.A.O and PIBIC scholarship to M.C.B); the Fundação de Amparo a Pesquisa do Estado de Minas Gerais-FAPEMIG/Brazil (Grant to C.A.O.); and the Coordenação de Aperfeiçoamento de Pessoal de Nível Superior-CAPES/Brazil (Doctoral fellowship to G.H.C·S and Masters fellowship to B.T.M and H.W.G).

The authors thank the Center of Microscopy, Center for Acquisition and Processing of Images, and Center for Gastrointestinal Biology of the UFMG for providing the equipment and technical support for experiments involving electron, light, and confocal microscopy. The authors are also grateful to Dr. Enio Ferreira for his contribution in identifying pituitary adenomas and all anonymous referees for their helpful suggestions.

Author contributions

Study design: GHCS HWG CAO. Execution of experiments: GHCS HWG BTM MCB MJT. Data collection and analysis: GHCS HWG BTM CAO. Technical and intellectual support: HRC GABM CAO. Manuscript drafting: GHCS HWG BTM CAO. All the authors have revised and approved the final version of the manuscript.

Declaration of competing interest

The authors declare that there are no conflicts of interest.

Appendix A. Supplementary data

Supplementary data to this article can be found online at https://doi.org/10.1016/j.lfs.2019.117149.

References

[1] C.K. Zhou, D.P. Check, J. Lortet-Tieulent, M. Laversanne, A. Jemal, J. Ferlay, F. Bray, M.B. Cook, S.S. Devesa, Prostate cancer incidence in 43 populations worldwide: an analysis of time trends overall and by age group, Int. J. Cancer 138 (2016) 1388–1400.
[2] F. Bray, J. Ferlay, I. Soerjomataram, R.L. Siegel, L.A. Torre, A. Jemal, Global cancer statistics 2018: GLOBOCAN estimates of incidence and mortality worldwide for 36 cancers in 185 countries, CA Cancer J. Clin. 68 (2018) 394–424.
[3] J.T. Isaacs, The aging ACI/Seg versus Copenhagen male rat as a model system for the study of prostatic carcinogenesis, Cancer Res. 44 (1984) 5785–5796.
[4] M. Krieg, R. Nass, S. Tunn, Effect of aging on endogenous level of 5 alpha-dihydrotestosterone, testosterone, estradiol, and estrone in epithelium and stroma of normal and hyperplastic human prostate, J. Clin. Endocrinol. Metab. 77 (1993) 375–381.
[5] P.P. Banerjee, S. Banerjee, J.M. Lai, J.D. Strandberg, B.R. Zirkin, T.R. Brown, Age-dependent and lobe-specific spontaneous hyperplasia in the brown Norway rat prostate, Biol. Reprod. 59 (1998) 1163–1170.
[6] M. Morais-Santos, A.E. Nunes, A.G. Oliveira, J.D. Moura-Cordeiro, G.A. Mahecha, M.C. Avellar, C.A. Oliveira, Changes in estrogen receptor ERbeta (ESR2) expression without changes in the estradiol levels in the Prostate of aging rats, PLoS One 10 (2015) e0131901.
[7] A. Vermeulen, R. Rubens, L. Verdonck, Testosterone secretion and metabolism in old age, Acta Endocrinol. Suppl. (Copenh) 152 (1971) 23.
[8] Y. Shibata, K. Ito, K. Suzuki, K. Nakano, Y. Fukabori, R. Suzuki, Y. Kawabe, S. Honma, H. Yamanaka, Changes in the endocrine environment of the human prostate transition zone with aging: simultaneous quantitative analysis of prostatic sex steroids and comparison with human prostatic histological composition, Prostate 42 (2000) 45–55.
[9] R.L. Noble, The development of prostatic adenocarcinoma in Nb rats following prolonged sex hormone administration, Cancer Res. 37 (1977) 1929–1933.
[10] R.L. Noble, Production of Nb rat carcinoma of the dorsal prostate and response of estrogen-dependent transplants to sex hormones and tamoxifen, Cancer Res. 40 (1980) 3547–3550.
[11] R.L. Noble, Prostate carcinoma of the Nb rat in relation to hormones, Int. Rev. Exp. Pathol. 23 (1982) 113–159.
[12] J.R. Drago, The induction of NB rat prostatic carcinomas, Anticancer Res. 4 (1984) 255–256.
[13] I. Leav, S.M. Ho, P. Ofner, F.B. Merk, P.W. Kwan, D. Damassa, Biochemical alterations in sex hormone-induced hyperplasia and dysplasia of the dorsolateral prostates of Noble rats, J. Natl. Cancer Inst. 80 (1988) 1045–1053.
[14] M.C. Bosland, H. Ford, L. Horton, Induction at high incidence of ductal prostate adenocarcinomas in NBL/Cr and Sprague-Dawley Hsd:SD rats treated with a combination of testosterone and estradiol-17 beta or diethylstilbestrol, Carcinogenesis 16 (1995) 1311–1317.
[15] N. Ozten, K. Vega, J. Liehr, X. Huang, L. Horton, E.L. Cavalieri, E.G. Rogan, M.C. Bosland, Role of estrogen in androgen-induced prostate carcinogenesis in NBL rats, Horm Cancer 10 (2019) 77–88.
[16] E. Nascimento-Goncalves, A.I. Faustino-Rocha, F. Seixas, M. Ginja, B. Colaco, R. Ferreira, M. Fardilha, P.A. Oliveira, Modelling human prostate cancer: rat models, Life Sci. 203 (2018) 210–224.
[17] S.A. Shain, B. McCullough, A. Segaloff, Spontaneous adenocarcinomas of the ventral prostate of aged A X C rats, J. Natl. Cancer Inst. 55 (1975) 177–180.
[18] T. Suwa, A. Nyska, J.C. Peckham, J.R. Hailey, J.F. Mahler, J.K. Haseman, R.R. Maronpot, A retrospective analysis of background lesions and tissue accountability for male accessory sex organs in Fischer-344 rats, Toxicol. Pathol. 29 (2001) 467–478.
[19] D. Cunningham, Z. You, In vitro and in vivo model systems used in prostate cancer research, J. Biol. Methods 2 (2015).
[20] T.R. Tennant, H. Kim, M. Sokoloff, C.W. Rinker-Schaeffer, The Dunning model, Prostate 43 (2000) 295–302.
[21] M. Pollard, Spontaneous prostate adenocarcinomas in aged germfree Wistar rats, J. Natl. Cancer Inst. 51 (1973) 1235–1241.
[22] S.B. Shappell, G.V. Thomas, R.L. Roberts, R. Herbert, M.M. Ittmann, M.A. Rubin, P.A. Humphrey, J.P. Sundberg, N. Rozengurt, R. Barrios, et al., Prostate pathology of genetically engineered mice: definitions and classification. The consensus report from the Bar Harbor meeting of the Mouse Models of Human Cancer Consortium Prostate Pathology Committee, Cancer Res. 64 (2004) 2270–2305.
[23] D. Creasy, A. Bube, E. de Rijk, H. Kandori, M. Kuwahara, R. Masson, T. Nolte, R. Reams, K. Regan, S. Rehm, et al., Proliferative and nonproliferative lesions of the rat and mouse male reproductive system, Toxicol. Pathol. 40 (2012) 40S–121S.
[24] G.H. Campolina-Silva, B.T. Maria, G.A.B. Mahecha, C.A. Oliveira, Reduced vitamin D receptor (VDR) expression and plasma vitamin D levels are associated with aging-related prostate lesions, Prostate 78 (2018) 532–546.
[25] S.C. Taylor, T. Berkelman, G. Yadav, M. Hammond, A defined methodology for reliable quantification of Western blot data, Mol. Biotechnol. 55 (2013) 217–226.
[26] P. Mak, I. Leav, B. Pursell, D. Bae, X. Yang, C.A. Taglienti, L.M. Gouvin, V.M. Sharma, A.M. Mercurio, ERbeta impedes prostate cancer EMT by destabilizing HIF-1alpha and inhibiting VEGF-mediated snail nuclear localization: implications for Gleason grading, Cancer Cell 17 (2010) 319–332.
[27] M.I. Khan, A. Hamid, V.M. Adhami, R.K. Lall, H. Mukhtar, Role of epithelial mesenchymal transition in prostate tumorigenesis, Curr. Pharm. Des. 21 (2015) 1240–1248.
[28] J. Colditz, B. Rupf, C. Maiwald, A. Baniahmad, Androgens induce a distinct response of epithelial-mesenchymal transition factors in human prostate cancer cells, Mol. Cell. Biochem. 421 (2016) 139–147.
[29] M. Pollard, The Lobund-Wistar rat model of prostate cancer, J. Cell. Biochem. Suppl. 16H (1992) 84–88.
[30] M. Morais-Santos, H. Werneck-Gomes, G.H. Campolina-Silva, L.C. Santos, G.A.B. Mahecha, R.A. Hess, C.A. Oliveira, Basal cells show increased expression of aromatase and estrogen receptor alpha in prostate epithelial lesions of male aging rats, Endocrinology 159 (2018) 723–732.
[31] A. Rivenson, J. Silverman, The prostatic carcinoma in laboratory animals: a bibliographic survey from 1900 to 1977, Investig. Urol. 16 (1979) 468–472.
[32] T. Suwa, A. Nyska, J.K. Haseman, J.F. Mahler, R.R. Maronpot, Spontaneous lesions in control B6C3F1 mice and recommended sectioning of male accessory sex organs, Toxicol. Pathol. 30 (2002) 228–234.
[33] G. Reznik, M.H. Hamlin 2nd, J.M. Ward, S.F. Stinson, Prostatic hyperplasia and neoplasia in aging F344 rats, Prostate 2 (1981) 261–268.
[34] J.M. Ward, G. Reznik, S.F. Stinson, C.P. Lattuada, D.G. Longfellow, T.P. Cameron, Histogenesis and morphology of naturally occurring prostatic carcinoma in the ACI/segHapBR rat, Lab. Investig. 43 (1980) 517–522.
[35] A.M. De Marzo, M.C. Haffner, T.L. Lotan, S. Yegnasubramanian, N.W.G. Premalignancy in Prostate Cancer, Rethinking what we know, Cancer Prev. Res. (Phila.) 9 (2016) 648–656.
[36] S. Gadkar, S. Nair, S. Patil, S. Kalamani, A. Bandivdekar, V. Patel, U. Chaudhari, G. Sachdeva, Membrane-initiated estrogen signaling in prostate cancer: a route to epithelial-to-mesenchymal transition, Mol. Carcinog. 58 (2019) 2077–2090.
[37] S.J. Ellem, H. Wang, M. Poutanen, G.P. Risbridger, Increased endogenous estrogen synthesis leads to the sequential induction of prostatic inflammation (prostatitis)

and prostatic pre-malignancy, Am. J. Pathol. 175 (2009) 1187–1199.
[38] J.A.F. Silva, A. Bruni-Cardoso, T.M. Augusto, D.M. Damas-Souza, G.O. Barbosa, S.L. Felisbino, D.R. Stach-Machado, H.F. Carvalho, Macrophage roles in the clearance of apoptotic cells and control of inflammation in the prostate gland after castration, Prostate 78 (2018) 95–103.
[39] M.V. Scalerandi, N. Peinetti, C. Leimgruber, M.M. Cuello Rubio, J.P. Nicola, G.B. Menezes, C.A. Maldonado, A.A. Quintar, Inefficient N2-like neutrophils are promoted by androgens during infection, Front. Immunol. 9 (2018) 1980.
[40] H. Abdelmoteleb, F. Rashed, A. Hawary, Management of prostate abscess in the absence of guidelines, Int. Braz. J. Urol. 43 (2017) 835–840.
[41] K.M. Lau, N.N. Tam, C. Thompson, R.Y. Cheng, Y.K. Leung, S.M. Ho, Age-associated changes in histology and gene-expression profile in the rat ventral prostate, Lab. Investig. 83 (2003) 743–757.
[42] J.C. Rinaldi, L.A. Justulin Jr., L.M. Lacorte, C. Sarobo, P.A. Boer, W.R. Scarano, S.L. Felisbino, Implications of intrauterine protein malnutrition on prostate growth, maturation and aging, Life Sci. 92 (2013) 763–774.
[43] Heckel NJ, Kretschmer. Carcinoma of the prostate treated with diethylstilbestrol. JAMA 1942; 119: 1087.
[44] M.S. Lucia, D.G. Bostwick, M. Bosland, A.T.K. Cockett, D.W. Knapp, I. Leav, M. Pollard, C. Rinker-Schaeffer, T. Shirai, B.A. Watkins, Workgroup I: rodent models of prostate cancer, Prostate 36 (1998) 49–55.